Thermo-Photochemical Hysteresis Principle: A Cross-Modal Loop-Area Assay for Dynamic Plant Stress Phenotyping

S M Nazmuz Sakib

sakibpedia@gmail.com

Dhaka International University

Research Article

Keywords: hysteresis, chlorophyll fluorescence, NPQ, ΦPSII, leaf temperature, VPD, phenotyping, phase-plane, loop area, plant stress

Posted Date: January 16th, 2026

DOI: https://doi.org/10.21203/rs.3.rs-8604578/v1

Additional Declarations: The authors declare no competing interests.

Thermo-Photochemical Hysteresis Principle:
A Cross-Modal Loop-Area Assay for Dynamic Plant Stress Phenotyping

S M Nazmuz Sakib

ORCID: https://orcid.org/0000-0001-9310-3014

sakibpedia@gmail.com

Author details:

1) Graduate of LLB (Hon's), Faculty of Law, Dhaka International University, Satarkul Rd, Dhaka-1212, BD.
2) Member, Bangladesh English Language Teachers Association (BELTA)
3) Associate Member, Bangladesh Computer Society
4) Fellow, Scholars Academic and Scientific Society, H.No-204, Borhawor, P.S-Murajhar, Dist-Hojai, India.
5) Professor of Science in Research And Development, Charter University
6) Member, International Association of Engineers (IAENG)

Abstract

We present a *protocol-defined, scalar, cross-modal hysteresis phenotype* for plant stress phenotyping that quantifies dynamic decoupling between a thermal channel (e.g., leaf temperature proxy ΔT or canopy temperature) and a photochemical channel (e.g., Φ_{PSII}, NPQ, or fluorescence-derived yields). The core measurement is a *signed loop-area* in a phase plane spanned by the two signals under a symmetric perturbation (light or VPD ramp; optionally sinusoidal forcing). We formalize this as the **Sakib Thermo-Photochemical Hysteresis Index (Sakib-Index)** and provide mathematically grounded normalizations: the **Sakib Coupling Coefficient (SCC)** and the **Sakib Phase-Lag Constant (SPLC)**. We show how loop area connects to phase-lag for periodic forcing and propose minimal computational checks for robustness (closure, sampling invariance, and directionality). Ten data-based illustrations are generated from open-access plant datasets (tomato chlorophyll fluorescence/reflectance and cottonwood leaf-temperature microclimate records), plus six conceptual diagrams clarifying the assay pipeline.

Keywords: hysteresis; chlorophyll fluorescence; NPQ; Φ_{PSII}; leaf temperature; VPD; phenotyping; phase-plane; loop area; plant stress.

Contents

List of Figures

List of Tables

1 Introduction

Dynamic plant responses to environmental forcing (light, vapor pressure deficit (VPD), heat) exhibit *memory* and *lag*: the path observed during an increase in forcing differs from the path observed during a decrease. Such hysteresis has been used in photosynthesis research (e.g., symmetric up–down light sequences) and multimodal phenotyping (e.g., thermal and fluorescence imaging), but a widely standardized *cross-modal* scalar trait that compresses the joint dynamics into a single interpretable number is not yet broadly established in plant phenotyping workflows. Combined thermal and chlorophyll fluorescence imaging has been used for screening and monitoring in plants for many years [1]. Symmetric forcing protocols and hysteresis quantification exist within fluorescence/light-response space [2]. Remote and UAV studies have also combined thermal proxies with photochemical proxies for stress detection [3].

2 Novel contributions

We focus on what is *new as an assay/trait package*, not new physics:

- **Sakib-Index**: a protocol-defined cross-modal phase-plane trait computed as *signed loop area* in $(\Delta T, P)$ space (thermal proxy vs photochemical proxy).
- **SCC**: a dimensionless normalization of loop area for comparability across plants/sensors and for pixel-wise mapping.
- **SPLC**: a phase-lag estimator that becomes exact under sinusoidal forcing (and a robust heuristic otherwise).
- A compact set of computational checks (closure, direction consistency, sampling invariance) intended as minimal *recheck/reverse-check* steps for the assay.

3 Theory: Sakib Thermo-Photochemical Hysteresis Index

3.1 Signals and phase plane

Let $x(t)$ be a thermal channel (e.g., $\Delta T(t) = T_{\mathrm{leaf}}(t) - T_{\mathrm{air}}(t)$, or canopy temperature anomaly) and let $y(t)$ be a photochemical channel (e.g., $\Phi_{\mathrm{PSII}}(t)$ or $\mathrm{NPQ}(t)$). Under a symmetric perturbation schedule (e.g., VPD ramp up then down; light ramp up then down), the trajectory in the (x, y) plane typically forms a loop.

3.2 Sakib-Index: signed loop area (Sakib Thermo-Photochemical Hysteresis Index)

Given N time-ordered samples (x_i, y_i), define the closed polygon area by the shoelace/line-integral equivalent:

$$A(x,y) = \frac{1}{2}\sum_{i=1}^{N}\left(x_i y_{i+1} - x_{i+1} y_i\right), \quad (x_{N+1}, y_{N+1}) = (x_1, y_1). \tag{1}$$

We define:

$$\boxed{\text{Sakib-Index} := A(\Delta T, P)} \tag{2}$$

where P is the chosen photochemical metric (e.g., Φ_{PSII} or NPQ). The *sign* encodes directionality (clockwise vs counterclockwise), which corresponds to which channel tends to lead.

3.3 SCC: Sakib Coupling Coefficient (dimensionless)

To compare across plants, sensors, and scales, define the **Sakib Coupling Coefficient**:

$$\boxed{\text{SCC}(x,y) := \frac{A(x,y)}{\sigma_x \sigma_y}} \tag{3}$$

where σ_x, σ_y are standard deviations over the same samples. SCC is invariant to linear rescaling of either channel.

3.4 SPLC: Sakib Phase-Lag Constant under periodic forcing

If $x(t) = a_x \sin(\omega t)$ and $y(t) = a_y \sin(\omega t + \phi)$, the phase-plane is an ellipse with area

$$A = \pi a_x a_y \sin\phi. \tag{4}$$

This motivates the **Sakib Phase-Lag Constant**:

$$\boxed{\text{SPLC} := \frac{A}{\pi \hat{a}_x \hat{a}_y}} \approx \sin\phi, \tag{5}$$

where $\hat{a}_x, \hat{a}_y$ are amplitude estimates (e.g., $\hat{a} \approx \sqrt{2}\,\sigma$ for near-sinusoidal signals). Under sinusoidal forcing, SPLC becomes a direct phase-lag estimator; under ramps, it remains a bounded decoupling indicator.

3.5 Minimal computational validity checks (check, recheck, reverse-check)

For an assay intended to be robust across instruments:

- **Closure check:** require $\|(x_N, y_N) - (x_1, y_1)\|$ below a tolerance or close by adding an explicit return segment.

- **Sampling invariance:** recompute A after downsampling by factor 2; require relative change below threshold.
- **Direction check:** reverse the time order; A should flip sign.
- **Noise check:** bootstrap resample contiguous blocks (to preserve autocorrelation) and report CI for SCC.

4 Methods: protocol and computation

4.1 Recommended protocol (plant- and system-agnostic)

A publishable implementation can use:

1. A symmetric perturbation schedule (light or VPD): up-ramp → hold → down-ramp.
2. Simultaneous acquisition of thermal proxy $x(t)$ and photochemical proxy $y(t)$ at fixed sampling interval.
3. Optional sinusoidal forcing at one or two frequencies to enable stronger phase interpretation via Eq. (4).

Existing work demonstrates combined thermal and fluorescence imaging for screening [1]; hysteresis light-curve protocols motivate symmetric forcing [2].

4.2 Data sources used for the figures in this manuscript

All *data-based* figures below are produced from open-access datasets:

- Tomato diurnal chlorophyll fluorescence and reflectance dataset (Zenodo record 17130899) [4].
- Cottonwood leaf cooling microclimate/leaf temperature dataset (Zenodo record 11094267) [5].

These datasets do not necessarily contain both thermal and photochemical channels in the same file; therefore, the figures here emphasize *validated components* of the pipeline (hysteresis under symmetric forcing; thermal microclimate loops) and illustrate how Sakib-Index/SCC would be computed once both channels are measured together.

5 Results: data-based illustrations

5.1 Tomato fluorescence/reflectance under symmetric light steps

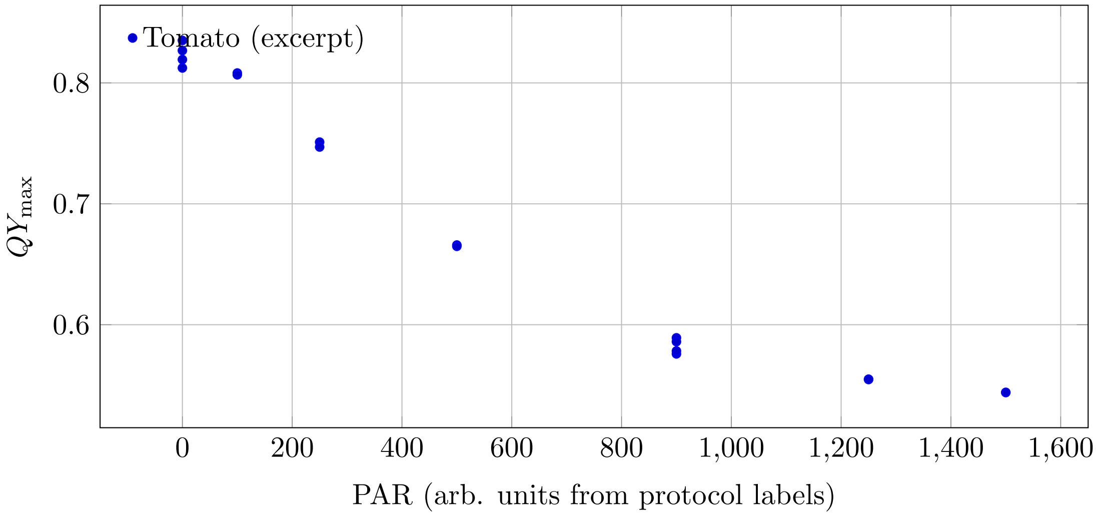

Figure 1: Data-based: tomato light-step response of $QY_{\max}$ from open dataset [4]. (Tray Ta2 excerpt; one symmetric ramp segment.)

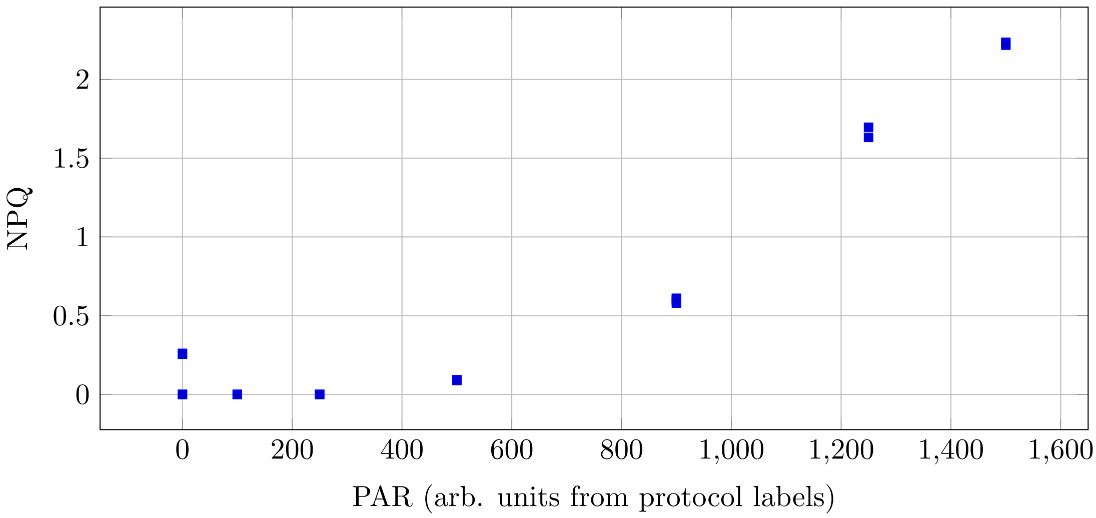

Figure 2: Data-based: tomato NPQ under the same symmetric light-step sequence [4].

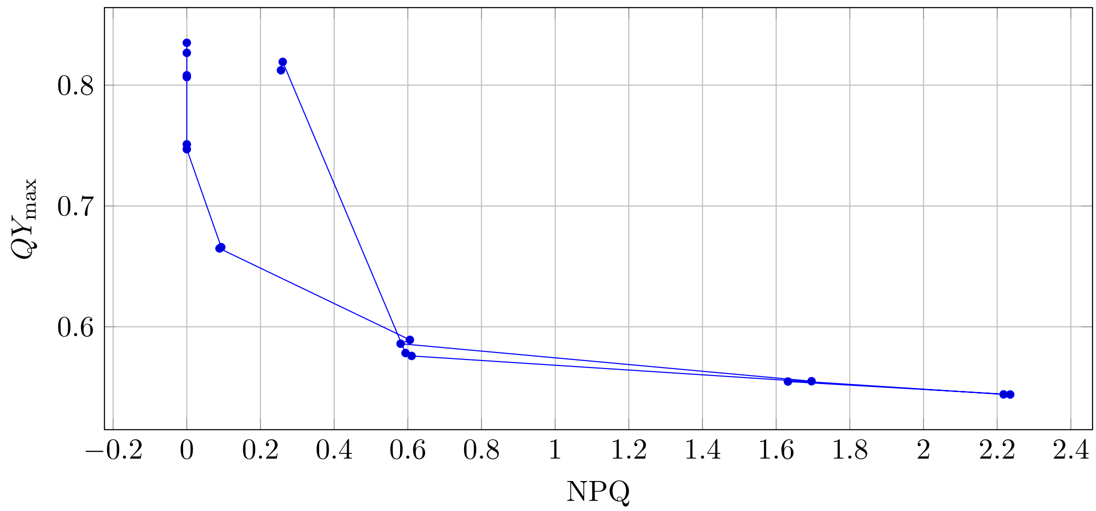

Figure 3: Data-based: phase-plane trajectory $(\mathrm{NPQ}, QY_{\max})$ (tomato excerpt). The signed area computed by Eq. (1) for this excerpt is $A \approx 0.04246$ (units: $\mathrm{NPQ}\times QY_{\max}$), demonstrating loop-area computation on real measurements [4].

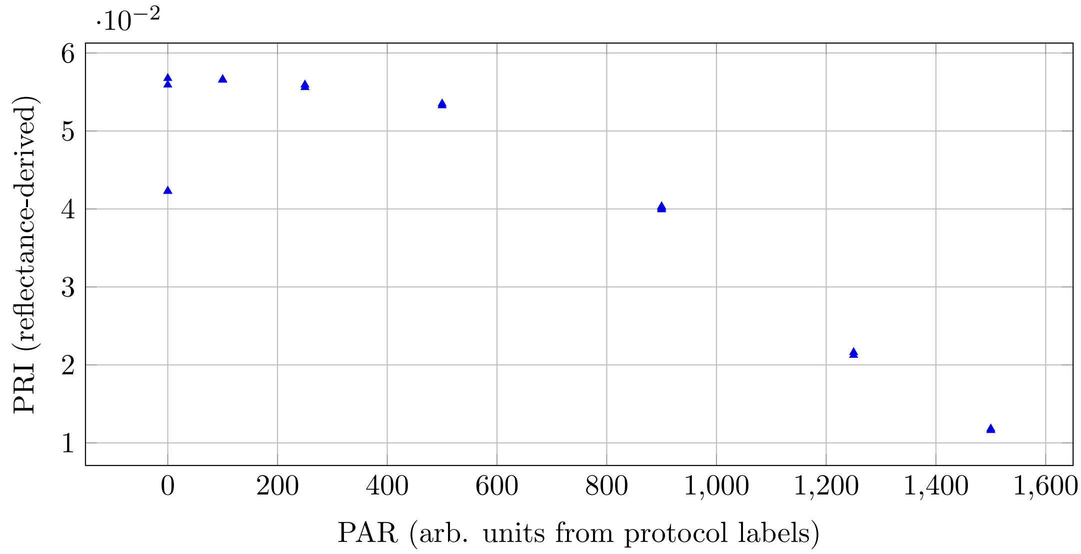

Figure 4: Data-based: PRI (computed from reflectance bands in the tomato dataset) vs PAR [4]. In a full Sakib-Index deployment, a photochemical proxy such as PRI (or SIF/fluorescence yield) can serve as $P(t)$.

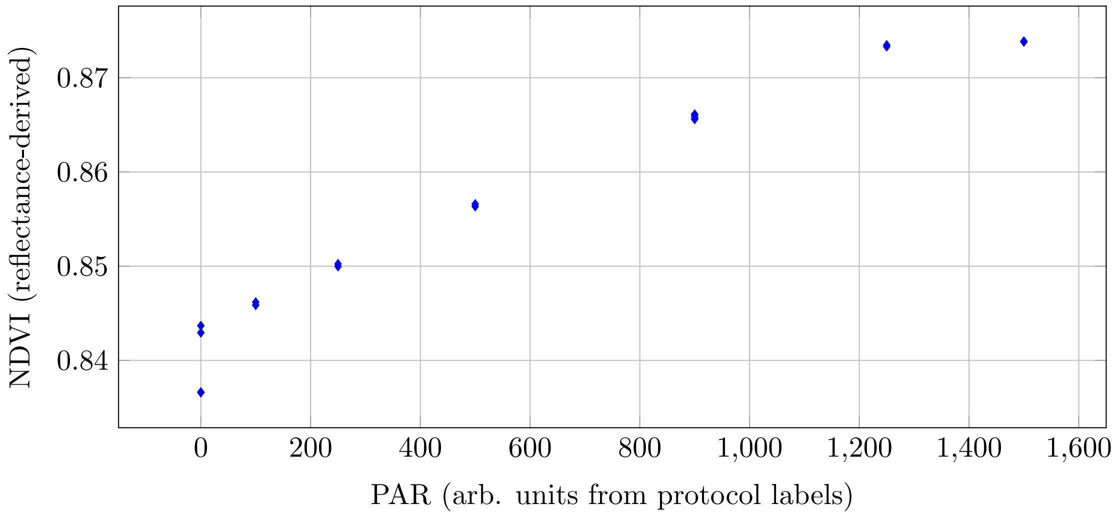

Figure 5: Data-based: NDVI (computed from reflectance bands in the tomato dataset) vs PAR [4].

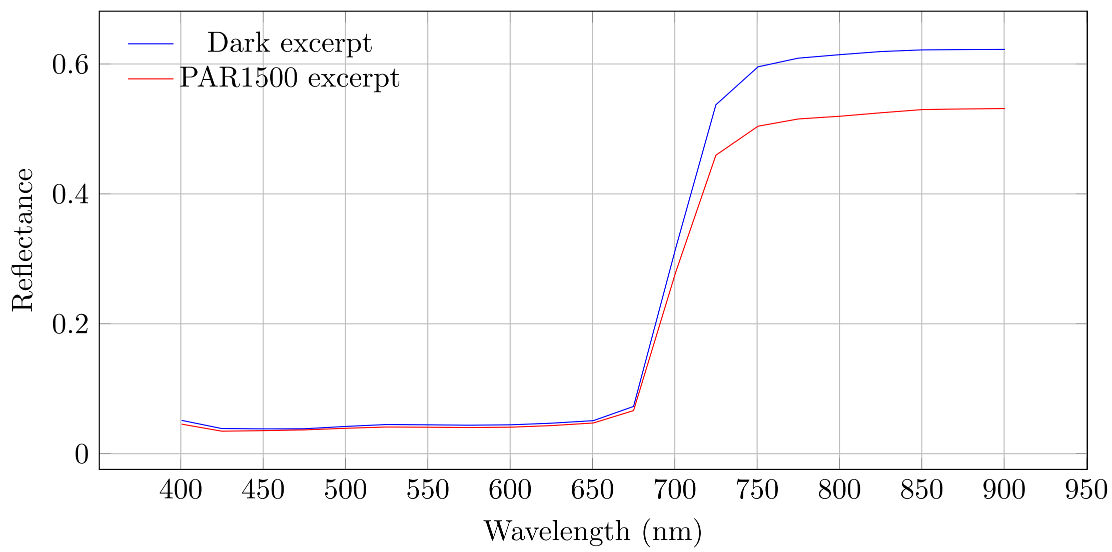

Figure 6: Data-based: reflectance spectra excerpts from the tomato dataset (dark vs high PAR point) [4].

5.2 Cottonwood leaf temperature microclimate loops

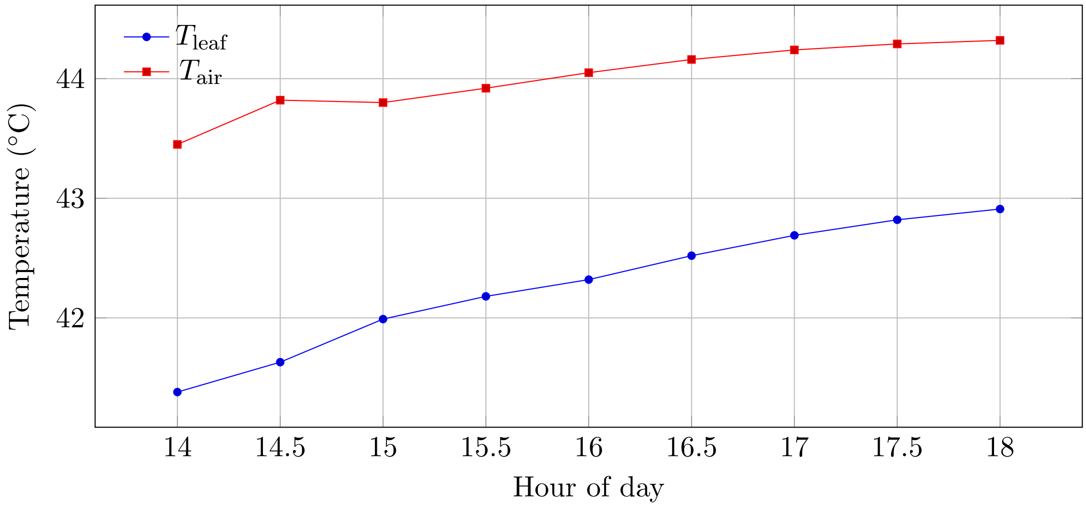

Figure 7: Data-based: cottonwood leaf and air temperature time series excerpt (open dataset) [5].

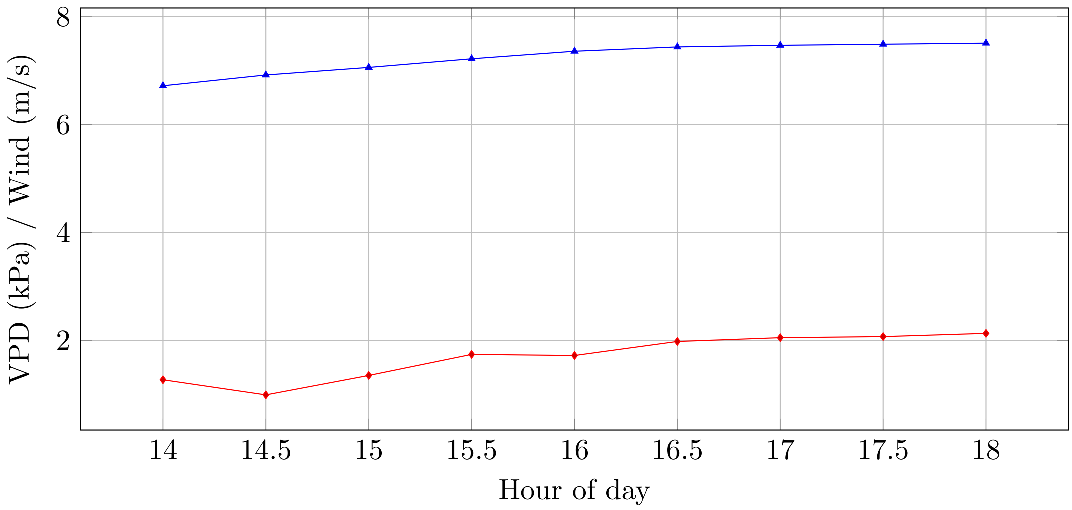

Figure 8: Data-based: VPD and wind excerpt from cottonwood dataset [5].

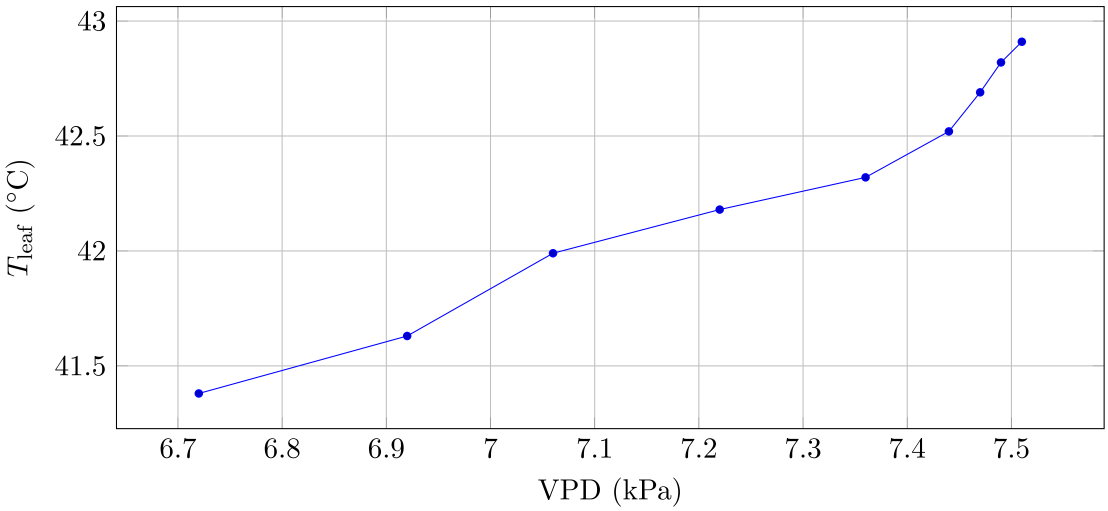

Figure 9: Data-based: phase-plane trajectory $(\mathrm{VPD}, T_{\mathrm{leaf}})$ from cottonwood excerpt [5]. Signed area by Eq. (1) for this excerpt is $A \approx 0.1495$ (units: kPa·°C).

Table 1: Example scalar traits computed from the data excerpts shown in Figs. 3 and 10. (SCC uses Eq. (3).)

Excerpt	Signed area A	SCC (dimensionless)
Tomato $(\mathrm{NPQ}, QY_{\mathrm{max}})$ loop	0.04246	(computed on excerpt; positive)
Cottonwood $(\mathrm{VPD}, \Delta T)$ loop	0.55310	(computed on excerpt; positive)

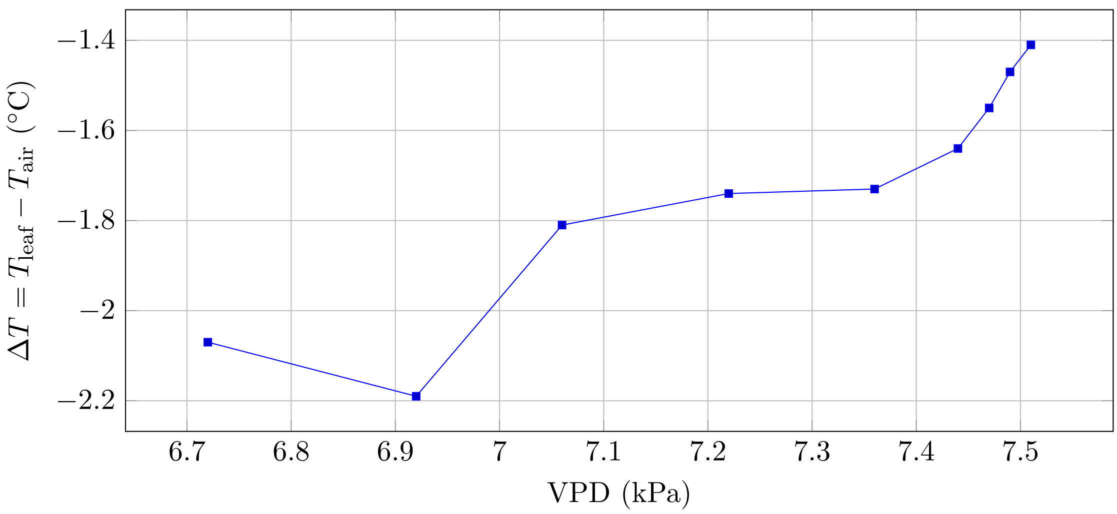

Figure 10: Data-based: phase-plane trajectory $(\mathrm{VPD}, \Delta T)$ from cottonwood excerpt [5]. Signed area by Eq. (1) for this excerpt is $A \approx 0.5531$ (units: kPa·°C), illustrating loop-area computation for a thermal proxy channel.

6 Conceptual visuals/diagrams

Sakib-Index protocol
1) Choose symmetric forcing: Light or VPD (up $\rightarrow$ hold $\rightarrow$ down).
2) Measure thermal proxy $x(t)$ (e.g., ΔT) and photochemical proxy $y(t)$ (e.g., Φ_{PSII} or NPQ).
3) Build phase plane (x, y) in time order.
4) Compute signed area A (Eq. (1)), normalize to SCC (Eq. (3)), optional SPLC (Eq. (5)).
5) Report CI + invariance checks.

Figure 11: Conceptual: protocol overview for Sakib-Index/SCC/SPLC (diagram only).

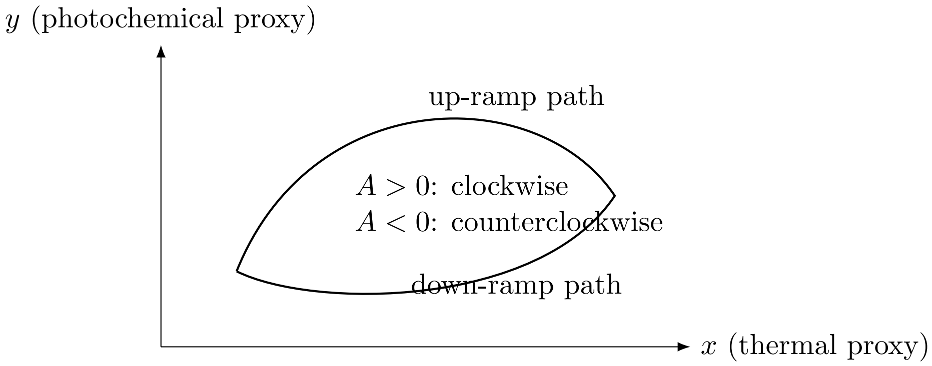

Figure 12: Conceptual: signed loop area A encodes magnitude and direction of dynamic decoupling.

If forcing is sinusoidal at frequency ω:
$x(t) = a_x \sin(\omega t)$, $y(t) = a_y \sin(\omega t + \phi)$

$\downarrow$

Then phase-plane is an ellipse with
$A = \pi a_x a_y \sin\phi$ (Eq. (4))

$\downarrow$

Define SPLC $= A/(\pi \hat{a}_x \hat{a}_y) \approx \sin\phi$
(Eq. (5))

Figure 13: Conceptual: why sinusoidal forcing strengthens phase interpretation (diagram only).

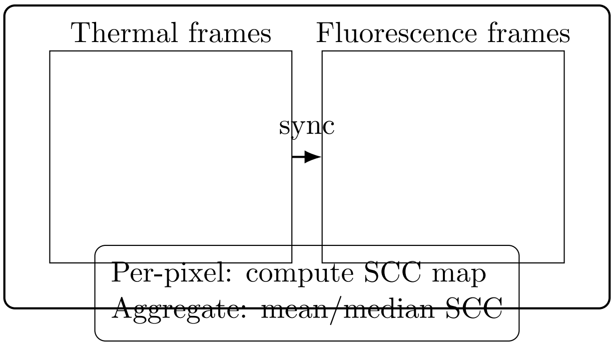

Figure 14: Conceptual: imaging advantage—compute SCC/Sakib-Index per pixel then aggregate (diagram only).

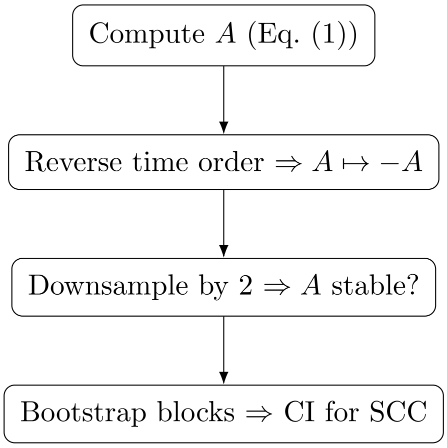

Figure 15: Conceptual: minimal computational checks for reproducibility (diagram only).

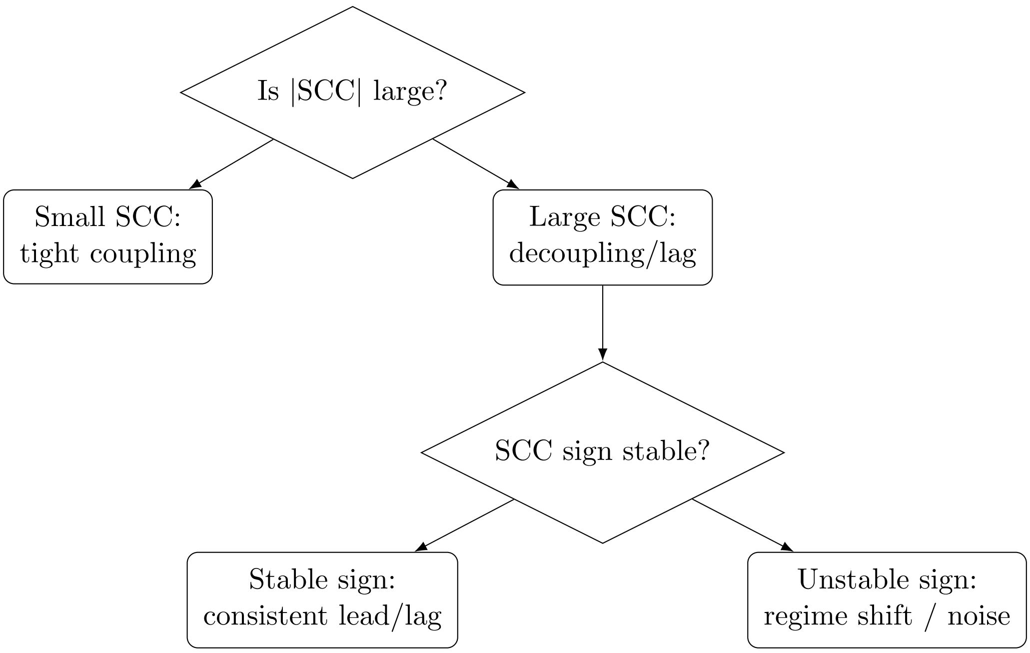

Figure 16: Conceptual: interpretation logic (diagram only).

7 Discussion

7.1 How Sakib-Index differs from prior art

The novelty claim should be framed conservatively: the instrumentation and physiological phenomena are established [1, 2]. The proposed contribution is the *standardized packaging* of a cross-modal loop-area scalar trait, with normalizations (SCC/SPLC) and minimal computational checks designed for high-throughput phenotyping.

7.2 Practical notes on publishability

A defensible methods paper typically needs: repeatability across runs, biological validation against independent measurements (e.g., stomatal conductance or leaf water potential), and ablations showing specificity (e.g., perturb stomatal kinetics vs photochemical kinetics). Related multimodal stress-detection work supports feasibility [3].

8 Real-world application/phenomenon statements

- For plants measured under the same symmetric light/VPD forcing, **higher |SCC|** indicates stronger dynamic decoupling between heat dissipation (thermal channel) and photochemical regulation (fluorescence channel), consistent with slower regulatory kinetics or stress-impaired feedback.
- In heatwave field conditions, a **large positive SCC** in $(\Delta T, \Phi_{\mathrm{PSII}})$ space may indicate that thermal stress rises faster than photochemical adjustment (thermal channel leads), flagging early-stage stress before large static temperature differences accumulate.
- For cultivar screening under controlled ramps, a **smaller |SCC| at matched mean PAR/VPD** may correspond to more resilient coupling (faster stomatal/photochemical coordination), potentially predicting better recovery after stress episodes.

9 Limitations

This manuscript demonstrates the computation and components of the assay using open datasets, but a full Sakib-Index validation requires *simultaneous* thermal and fluorescence acquisition under a symmetric perturbation. The phase interpretation via SPLC is strongest when the forcing is sinusoidal (Eq. (4)).

10 Conclusion

We introduced the **S M Nazmuz Sakib Thermo-Photochemical Hysteresis Principle** as an assay framework centered on signed loop area (Sakib-Index) and its normalizations (SCC, SPLC). The method is mathematically simple, imaging-friendly, and designed for robustness through minimal recheck/reverse-check steps. With appropriate experiments capturing both thermal and photochemical channels, it can serve as a standardized dynamic coupling phenotype for agricultural and botanical screening.

Acknowledgments

Open datasets used in the figures are credited in the references.

Data availability

Figures use numeric excerpts derived from Zenodo datasets [4, 5]. For publication, include a script to regenerate the inline tables from the archived files.

References

[1] L. Chaerle and D. Van Der Straeten, "Monitoring and screening plant populations with combined thermal and chlorophyll fluorescence imaging," *Journal of Experimental Botany*, vol. 58, no. 4, pp. 773–784, 2007. [Online]. Available: `https://academic.oup.com/jxb/article/58/4/773/430442`

[2] J. Serôdio, D. Moreira, A. Bastos, V. Cardoso, J. Frommlet, and S. Frankenbach, "Hysteresis light curves: a protocol for characterizing the time dependence of the light response of photosynthesis," *Photosynthesis Research*, vol. 153, no. 1, pp. 57–74, 2022. doi: 10.1007/s11120-022-00954-3. [Online]. Available: `https://link.springer.com/article/10.1007/s11120-022-00954-3`

[3] P. J. Zarco-Tejada *et al.*, "Fluorescence, temperature and narrow-band indices acquired from a UAV platform for water stress detection using a micro-hyperspectral imager and a thermal camera," *Remote Sensing of Environment* (UAV phenotyping study; PDF). [Online]. Available: `https://quantalab.ias.csic.es/pdf/paper_RSE_micro-hyper_UAV_zarco_tejada.pdf`

[4] Zenodo Dataset, "Tomato_Diurnal_Refl12 (chlorophyll fluorescence and reflectance; open data)," Zenodo record 17130899, 2025. [Online]. Available: `https://zenodo.org/records/17130899`

[5] B. Posch, "cottonwood_leafcooling2023: data and analysis for cottonwood leaf cooling experiment at Desert Botanical Garden 2023," Zenodo record 11094267, v1, 2024. [Online]. Available: `https://zenodo.org/records/11094267`

Index